molecular pharmaceutics

ARTICLE

pubs.acs.org/molecularpharmaceutics

A Comparative Study of Neural and Mesenchymal Stem Cell-Based Carriers for Oncolytic Adenovirus in a Model of Malignant Glioma

Atique U. Ahmed, Matthew A. Tyler, Bart Thaci, Nikita G. Alexiades, Yu Han, Ilya V. Ulasov, and Maciej S. Lesniak*

The Brain Tumor Center, The University of Chicago, Chicago, Illinois 60637

Supporting Information

ABSTRACT: Glioblastoma multiforme is a primary malignancy of the central nervous system that is universally fatal due to its disseminated nature. Recent investigations have focused on the unique tumor-tropic properties of stem cells as a novel platform for targeted delivery of anticancer agents to the brain. Neural stem cells (NSCs) and mesenchymal stem cells (MSCs) both have the potential to function as cell carriers for targeted delivery of a glioma restricted oncolytic virus to disseminated tumor due to their reported tumor tropism. In this study, we evaluated NSCs and MSCs as cellular delivery vehicles for an oncolytic adenovirus in the context of human glioma. We report the first preclinical comparison of the two cell lines and show that, while both stem cell lines are able to support therapeutic adenoviral replication intracellularly, the amount of virus released from NSCs was a log higher than the MSC ($p < 0.001$). Moreover, only virus loaded NSCs that were administered intracranially in an orthotopic glioma model significantly prolonged the survival of tumor bearing animals (median survival for NSCs 68.5 days vs 44 days for MSCs, $p < 0.002$). Loading oncolytic adenovirus into NSCs and MSCs also led to expression of both pro- and anti-inflammatory genes and decreased vector-mediated neuroinflammation. Our results indicate that, despite possessing a comparable migratory capacity, NSCs display superior therapeutic efficacy in the context of intracranial tumors. Taken together, these findings argue in favor of NSCs as an effective cell carrier for antiglioma oncolytic virotherapy.

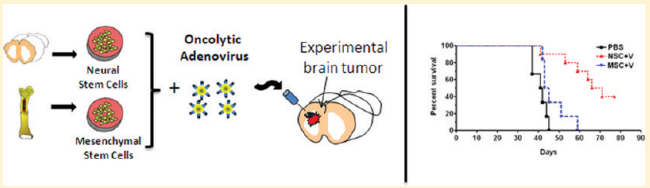

KEYWORDS: stem cell, mesenchymal stem cell, neural stem cell, oncolytic adenovirus, glioblastoma, cell carrier, virotherapy

INTRODUCTION

Glioblastoma multiforme (GBM) is both the most common and the most deadly primary tumor of the central nervous system. Despite numerous therapeutic advancements, the prognosis for patients afflicted with this disease has improved little in recent decades with a median survival that remains under 15 months.[1] The success of current therapies is limited in part due to the disseminated nature of these tumors. Furthermore, conventional radio- and chemotherapy regimes employed against CNS tumors carry with them severe toxicities toward healthy parenchyma that may culminate in potentially devastating consequences on patient's cognitive function.[2] Ultimately, the most effective treatment of these cancers will require the development of new methods able to target diffuse tumor microsatellites located significant distances away from the primary tumor focus while maintaining selectivity for diseased tissue and sparing healthy brain.

In the past decade, many *in vitro* and *in vivo* studies have demonstrated that stem cells possess an inherent tropism toward invasive malignancies within the brain, including glioblastoma.[3−6] These observations provided an impetus for the design of a targeted therapeutic delivery modality employing stem cells as a vehicle to track invasive tumor burden and selectively distribute anticancer agents to diseased areas. Many early preclinical studies investigating the tumor-homing capability of stem cells were performed in intracranial glioma models.[3,4,7] The infiltrative nature of this tumor and its propensity for distant spread make it an appropriate platform for such investigations. Before stem cell-based antiglioma therapy makes the ultimate transition into human clinical trials, however, it is crucial to identify the ideal therapeutic agent to be shepherded by these vectors.[8] Such an agent must simultaneously balance the need for maximal therapeutic efficacy with an impressive safety profile to ensure increased survival while minimizing complications. First, this agent must be highly potent; it must also possess maximal antitumor activity at low concentrations due to barriers imposed by a variety of immune, biochemical, and physiological mechanisms that will limit the number of transplanted stem cells able to migrate to diffuse tumor foci. The amplification of antitumor effects at target sites may be necessary to achieve clinical success. Second, any stem cell-based therapy should selectively target proliferating neoplastic cells while sparing normal CNS tissues.

Special Issue: Emerging Trends in Gene- and Stem-Based Combination Therapy

Received: March 31, 2011
Accepted: June 14, 2011
Revised: June 6, 2011
Published: June 30, 2011

One viable approach meeting these criteria is oncolytic virotherapy (OV).[8] This is a novel approach in which viruses are genetically modified to selectively replicate in tumor cells. OVs are able to replicate selectively in tumor cells and thus may amplify therapeutic genes at tumor sites. Furthermore, once an OV releases from its carrier at target sites, it can distinguish tumor from normal tissues and induce tumor cell specific oncolysis. During the past two decades, a number of promising oncolytic viruses (OVs) have demonstrated antitumor activity in both preclinical and clinical settings.[9,10] Despite promising results, two major hurdles remain preventing the advancement of OV based therapies: the host antiviral immune response and inefficient viral distribution away from the tumor site.

The immune system is wired to mount a defense against foreign invaders regardless of their intentions. As a result, most of the oncolytic virus administered at a tumor site fails to persist as free-floating particles[11] and to target metastatic tumor burden effectively. Early *in vivo* experiments with OVs revealed that infected virus-producing cells could also mediate antitumor activity when administered in place of naked virus.[12] This led to the hypothesis that producer cells can be used to shield a therapeutic virus from the host immune system. Our lab along with others has shown that different lineages of stem cells can be used as carriers for the stealth delivery of an oncolytic adenovirus *in vivo* for antiglioma therapy.[5,7,13] Two classes of stem cells have been evaluated most extensively as cell carriers for anticancer therapies: neural and mesenchymal stem cells. Neural stem cells (NSCs), derived from fetal, neonatal, or postnatal tissues,[14] are multipotent and capable of differentiation into three major types of CNS cells: neurons, astrocytes and oligodendrocytes.[15] Mesenchymal stem cells (MSCs), derived from bone marrow, are also multipotent cells. These cells differentiate into a variety of cells destined to become mesenchymal tissues, including osteoblasts, chondrocytes, and adipocytes.[16−18] In animal models, both of these stem cell populations have demonstrated their ability to travel great distances in the brain and home to disseminated tumor foci.[19] However, quantitative or qualitative comparison of NSCs and MSCs as carriers for the oncolytic virus has yet to be done.

Here, we report the first preclinical comparison of NSCs and MSCs as cell delivery vehicles for oncolytic virotherapy in the context of human glioma. Our results indicate that, despite possessing comparable migratory capacity, NSCs display superior migratory specificity toward intracranial glioma. Furthermore, despite the fact that both stem cell lines were able to support oncolytic adenoviral replication effectively, virus loaded into NSCs administered intracranially in an orthotopic glioma model significantly prolonged survival vs virus loaded MSCs. Evidence presented in this report further supports the notion that stem cell-based cell carriers can be utilized as a targeted delivery vehicle for antiglioma oncolytic virotherapy.

MATERIALS AND METHODS

Cell Culture and Establishment of Fluorescent-Labeled Cell Lines. The U87MG, U118MG, N10, U251, A172 and U373 human glioma cell lines were purchased from the American Type Culture Collection (Manassas, VA, USA) and maintained in MEM (minimum essential medium) (HyClone, Thermo Fisher Scientific, Waltham, MA, USA) containing 2% penicillin−streptomycin antibiotic (Cellgro, Mediatech, Inc., Manassas, VA, USA) and 10% fetal bovine serum (FBS; Atlanta Biologicals, Lawrenceville, GA, USA). All cells (including NSCs and MSCs) were grown in a humidified atmosphere, with 5% CO_2 and 37 °C conditions. U87MG, U118MG, and human MSCs were subcultured for experimentation using 1 mL/10^6 cells 0.25% Trypsin/2.21 mM EDTA solution (Mediatech Inc.; cat. no. 25-053-CI). Trypsin activity was quenched using the appropriate media for each cell type. Cells were then washed at 300 relative centrifugal force (rcf) and plated at the indicated densities.

Human primary brain tumor specimens (GBM1, GBM2) were obtained from patients undergoing surgery in accordance with a protocol approved by the Institutional Review Board at the University of Chicago. Tumor specimens were confirmed as World Health Organization grade IV malignant glioma by an attending neuropathologist. All human tissue specimens were treated with 1% hyaluronidase (Sigma-Aldrich, St. Louis, MO, USA) and 2% collagenase (Sigma-Aldrich) enzymes and subsequently minced through 70 μm strainers. After several washings in phosphate-buffered saline (PBS) solution, cells were then cultured in flasks containing neural basal media (NBM) (Invitrogen) supplemented with 100 μg mL^{-1} ampicillin/streptomycin and 20 ng mL^{-1} each of epidermal growth factor (Millipore, Billerica, MA, USA) and basic fibroblast growth factor (Millipore). Cells were maintained in a humidified atmosphere containing 5% CO_2 at 37 °C.

Human NSCs (ReNCell) were obtained from Millipore and maintained according the manufacturer's protocol. Briefly, these NSCs were isolated from the cortical region of 14-week-old fetal tissue and immortalized by retroviral transduction and insertion of the *c-myc* gene. Cells were characterized according to their expression of nestin, SOX-2, CD133 and CD44 (data not shown) stem cell markers. Subculture of human NSCs for experimentation was conducted as follows: tissue culture plastic dishes were coated with laminin (Sigma) at a concentration of 20 μg mL^{-1} in serum-free DMEM in 37 °C and 5% CO_2 atmospheric conditions 4 h before NSC plating. NSCs were detached from plastic dishes using 1 mL/10^6 cells of Accutase (Millipore), centrifuged at 300 rcf for 5 min, resuspended in ReNCell NSC Maintenance Medium (Millipore), supplemented with 20 ng mL^{-1} basic fibroblast growth factor (Millipore) and 20 ng mL^{-1} epidermal growth factor (Millipore) and seeded at the indicated cell densities.

The three stable, fluorescently labeled cell lines, U87-GFP, MSC-mCherry, and NSC-mCherry,[20] were established as described earlier.[21] Briefly, cells were seeded at a density of 5 × 10^4 cells/well (or 50−60% confluency) in six-well plastic culture dishes (BD, Franklin Lakes, NJ, USA). One day after plating, cells were incubated for 24 h with replication-deficient lentiviral vectors containing GFP (U87MG) or mCherry (NSC, MSC) expression cassettes. After 48 h, medium was replaced with fresh culture medium appropriate for each cell type containing 1 μg mL^{-1} Puromycin (Sigma) for the establishment of stable clonal populations. Selected populations were screened by FACS to verify mCherry and GFP expression.

hMSC cells of male origin were obtained from Cambrex (Walkersville, MD, http://www.cambrex.com; Lonza, Walkersville, MD, http://www.lonza.com) and characterized using CD105-, CD166-, CD29-, and CD44-positive cellular markers. Isolated cells were then expanded in MesenPro RS growth medium (12746-012; Gibco, Grand Island, NY, http://www.invitrogen.com) supplemented with 20% fetal bovine serum (FBS) (Atlanta Biologicals, Lawrenceville, GA, http://www.atlantabio.com), 1% penicillin/streptomycin (Gibco), 4 ng/mL basic fibroblast growth factor (R&D Systems Inc., Minneapolis,), and 0.25% Fungizone (Gibco) in a 37 °C, 5% CO_2 incubator.

Viral Vectors. The replication-competent adenoviral vectors, AdWT, CRAd-CXCR4−5/3, CRAd-CXCR4-RGD, CRAd-CXCR4-pk7, CRAd-S-RGD, CRAd-S-5/3 and CRAd-S-pk7, retain the wild-type *E1A* gene, which controls viral replication. AdWT is the wild-type Ad5. CXCR4-modified vectors (CRAd-CXCR4−5/3, CRAd-CXCR4-RGD and CRAd-CXCR4-pk7) or *survivin*-modified vectors (CRAd-S-5/3, CRAd-S-RGD CRAd-S-pk7) contain the wild-type Ad replication protein, *E1A*, under the control of either human *CXCR4* or *survivin* promoters. These vectors were created by homologous recombination between a shuttle plasmid containing either the human *CXCR4* or *survivin* promoter upstream of the viral *E1A* gene. Shuttle plasmids containing these regions were homologously recombined into adenoviral plasmids containing different modifications in the Ad fiber structure, such as an RGD incorporation into HI loop of wild-type fiber protein, a polylysine (pk7) incorporation into the C terminus of the wild-type fiber knob protein, or complete replacement of the type 5 fiber knob protein for knob protein from the type 3 Ad.[22−24]

Analysis of Viral Replication. To detect the level of viral replication by quantitative PCR, NSCs and MSCs were plated at a density of 2.5×10^4 cells/well in 24-well plastic tissue culture dishes. The next day, cells were infected with 1 infectious unit/cell of AdWT, AdRGD, Ad5/3, CRAd-CXCR4−5/3, CRAd-CXCR4-RGD, CRAd-CXCR4-pk7, CRAd-S-RGD, CRAd-S-5/3 or CRAd-S-pk7. After a one hour incubation period, virus-containing medium was removed, cells were washed with PBS, and a fresh portion of complete growth medium was added. Infected cells were harvested seven days postinfection. Total DNA was extracted from infected cells using a DNeasy Tissue Kit (Qiagen, Hilden, Germany) according to the manufacturer's protocol. Gene expression was quantified by real-time quantitative PCR using SYBR Green PCR Master Mix (Applied Biosystems, Foster City, CA, USA) and primers recognizing the viral *E1A* gene.[22] DNA amplification was carried out using an Opticon 2 system (Bio-Rad, Foster City, CA, USA), and the detection was performed by measuring the binding of the fluorescent dye, SYBR green. Each sample was run in triplicate. Results are presented as the average number of *E1A* copies per ng of DNA (*E1A* copies per ng of DNA).

We used the Adeno-X Rapid Titer Kit (Clontech) according to the manufacturer's protocol to titrate the levels of infectious viral progeny. Briefly, infectious progeny was released from the infected cells by collecting infected cells and medium from each group and subsequently subjecting them to three cycles of freeze−thawing. Cell lysates were then incubated with adherent HEK293 cells in serial 10-fold dilutions. Forty-eight hours later, the number of infectious units was calculated using the Adeno-X Rapid Titer Kit according to vendor recommendations. The titration unit (infectious units, iu) used by this protocol is similar to PFUs.

Crystal Violet Staining of Cell Monolayer. To assess the level of replicative cytotoxicity mediated by each CRAd, cell monolayers were washed twice with PBS followed by treatment with a 2% (w/v) methanolic solution of Gentian Violet (Ricca Chemicals). Plates were incubated at room temperature for 20 min in Gentian Violet staining solution. After staining, cells were washed thoroughly with lukewarm H_2O and air-dried for 24 h. Images were taken and analyzed using a ChemiDoc XRS imaging system (Bio-Rad).

Flow Cytometry Analysis of Protein Expression. Cells were labeled and analyzed for surface markers using a protocol that has been previously described.[7] Briefly, cells were permeabilized, fixed and stained on ice using the Cytofix/Cytoperm buffer (BD) according to the manufacturer's instructions. The following antibodies were used: rabbit polyclonal anti-GFAP (Abcam, Cambridge, MA; isotype, rat IgG_{2A}), APC-conjugated anti-CXCR4 IgG, alexa647-conjugated anti-VEGFR2 (Biolegend, San Diego, CA) and. Data were acquired and analyzed in Canto with CellQuest (Becton Dickinson, Franklin Lakes, NJ) and FlowJo (TreeStar, Ashland, OR) software.

Evaluation of NSC and MSC Migration and Viral Delivery *in Vitro*. To analyze the migratory capacity and oncolytic Ad delivery characteristics of NSC and MSC *in vitro*, we used a similar system to that described earlier,[22] with slight modification. To characterize the specificity of each stem cell carrier migration in response to glioma, we used a BD Biocoat Tumor Invasion System (BD Biosciences, http://www.bdbiosciences.com) containing BD Falcon Fluoroblock 24-Multiwell inserts (8-μm pore size; PET membrane) in accordance with the manufacturer's protocol. To aid in quantification of stem cell migration, fluorescently labeled MSC and NSC (described above) were used. The migration was characterized with respect to four different conditioned media and a negative control. Conditioned medium was obtained by culturing 1×10^5 cells of each cell type (GBM1, GBM2, U118MG, U87MG, N10, U51MG, A172, and U373MG) in serum-free/growth factor-free medium for 24 h, after which equal amounts of each conditioned medium were aliquoted in the bottom wells of the migration chamber to serve as a chemoattractant. For migration studies without Ad, NSC and MSC were plated in SF-MEM at a density of 5×10^4 cells/well. Twenty-four hours after plating NSC and MSC into the top insert, the number of migrating cells/field view was determined using an Olympus IX81 inverted microscope and MetaMorph software (Olympus, Tokyo, Japan). Cells were counted in three random field views/well (original objective: 10×). A total of 4 wells were used for each experimental condition (i.e., U118 = 4 wells).

For studies involving NSC- and MSC-mediated delivery of Ad, the same migration apparatus was used; however, NSC and MSC were loaded with different iu of CRAd-S-pk7 virus prior to being plated in the top chamber of the migration apparatus (5×10^4 cells/well). Instead of conditioned medium, U87 cells were plated in the bottom wells of the migration chamber in serum-free MEM supplemented with 20 ng/mL of basic fibroblast growth factor (bFGF) and epidermal growth factor to generate multicellular spheroids at a density of 5×10^4 cells/well two days before stem cells were plated in the top well of the migration chamber. The number of migrating cells was assessed as described above. Nonloaded NSC and MSC were plated in chambers immersed in serum-free MEM as a reference control. Nine days after plating loaded NSC and MSC in the top inserts, we quantified the number of infectious units in each of the bottom wells (4 wells/experimental condition) using the Adeno-X Rapid Titer Kit as described above. Cytotoxicity resulting from stem cell release of viral progeny was quantified by counting the number U87 glioma spheroids/field view (4× original objective) using the same Olympus IX81 inverted microscope. Three random field views per well were captured; there were a total of 4 wells per experimental condition.

Animal Studies. Male athymic/nude mice were obtained from Charles River Laboratory (Wilmington, MA, USA). Animals were cared for according to a study-specific animal protocol approved by the University of Chicago Institutional Animal Care and Use Committee. To detect loaded MSC and NSC *in vivo*, a total of 54 mice were injected with 3×10^5 U87 cells in 2.5 μL/mouse. Five days later, mice were randomly divided into 6 groups ($n = 9$ mice/group) which received the following injections: one group received an injection of 2.5 μL of PBS/mouse (Mock);

one group received an injection of 1×10^5 MSC in 2.5 μL of PBS/mouse (MSC); one group received an injection of 1×10^5 NSC in 2.5 μL of PBS/mouse (NSC); one group received 2.5 μL injections of 1×10^5 MSC infected with 5 IU of CRAd-S-pk7/mouse (MSC + V); and one group received 2.5 μL injections of 1×10^5 NSC infected with 5 IU of CRAd-S-pk7/mouse (NSC + V). U87 cells were detected via their expression of GFP, and NSC and MSC were detected by expression of the red fluorescent protein, mCherry.

Three mice from each group were sacrificed, and their brains were flash frozen in OCT solution at days six, nine, and twelve after the second round of injections (thirteen, sixteen, and nineteen days after U87 injection). Brains underwent serial coronal sectioning (6 μm/section) for a total of 20−25 slices per tissue, altogether spanning approximately 3 mm of brain tissue. Slices were fixed (4% paraformaldehyde, 10 min) and mounted on glass slides using Prolong Gold Antifade Reagent (Invitrogen). Fluorescent microscope analysis was performed using a Zeiss 200 M Axiovert inverted microscope (Carl Zeiss, Inc., Oberkochen, Germany). U87 tumors (GFP) were detected using a GFP optical band-pass filter, and MSC and NSC (mCherry) were detected using a Texas Red optical band-pass filter. Fluorescent images were analyzed and rendered for publication using Openlab v5.0 (Improvision, Coventry, England) and Adobe Photoshop CS2 (Adobe Systems, Inc., San Jose, CA).

To evaluate the therapeutic efficacy of NSCs loaded with OV virus, six groups of seven nude mice were implanted with U87 cells (5×10^5 cells in 2.5 μL of PBS/mouse into the right hemisphere as previously described). Five days post tumor implantation, mice received an intracranial, intratumoral injection of 5×10^5 stem cells loaded with OV (50 IU/cell) or an equal dose of naked virus. Both the stem cells were incubated with the oncolytic adenovirus for 2 h at room temperature, washed 3 times with PBS, resuspended in PBS (5×10^5 stem cells in 2.5 μL/mouse) and injected intratumorally in the tumor implanted right hemisphere. Animals losing ≥30% of their body weight or having trouble ambulating, feeding, or grooming were euthanized by CO_2 followed by cervical dislocation.

***In Vivo* Bioluminescence Imaging.** Mice were imaged for Fluc activity by intraperitoneal injection of D-luciferin (4.5 mg/animal in 150 μL of saline), and photon counts were recorded 10 min after D-luciferin administration by using a cryogenically cooled high efficiency charged-coupled device camera system (Xenogene).

Statistical Analysis. The statistical analysis presented was performed using GraphPad Prism Software v4.0 (GraphPad Software, Inc., La Jolla, CA). Where applicable, a standard independent two-sample *t*-test was applied. A *p*-value <0.05 was considered statistically significant. *** indicates a *p*-value <0.001; ** indicates a *p*-value <0.01; * indicates a *p*-value <0.05.

RESULTS

Permissiveness of Stem Cell Carriers for CRAd Replication. An optimal cell carrier for the delivery of an oncolytic virus must be capable of supporting amplification of its load via viral replication so that infectious virions can spread to diffusely infiltrated glioma tissue once delivered. To assess the permissiveness of each stem cell carrier, we conducted flow cytometry studies to evaluate the expression of adenovirus binding and internalization receptors, quantitative PCR to detect viral genome amplification, and toxicity and virus assembly studies.

Both stem cell lines exhibited expression of most Ad cell surface receptors tested (Figure 1A), which included the following: CAR (NSC, 99.9%; MSC, 94.1% cells positive), the primary binding receptor of the wild-type Ad5 virus; $\alpha_v\beta_3$ (NSC, 70.5%; MSC, 78.7%) and $\alpha_v\beta_5$ (NSC, 100%; MSC, 99.4%); CD44 (NSC, 88.1%; MSC, 96.8%) and CD138 (NSC, 70.3%; MSC, 77.2%), two of the many heparan sulfate proteoglycans targeted by pk7-modified CRAds.

Next, NSCs and MSCs were infected with a panel of different CRAds; seven days later, the levels of viral E1A DNA copies were measured by quantitative PCR (Figure 1B). Our results indicate that both MSCs and NSCs support genome amplification from a number of different CRAds. In both MSCs and NSCs, CRAds harboring survivin promoters that control viral replication demonstrated greater levels of viral replication than viruses possessing CXCR4 promoters upstream of the viral E1A gene, with CRAd-CXCR4-5/3 being the only exception. RGD- and pk7-modified CRAds demonstrated greater E1A levels in both NSCs and MSCs than CRAds expressing 5/3-knob modifications, despite both cell types exhibiting CD46 expression (data not shown). The wild-type Ad5 vector showed robust replication in both cell types. For subsequent comparative studies, we elected to use the CRAd-S-pk7 vector, due to its similar high level of E1As in both MSCs and NSCs.

We conducted crystal violet toxicity studies and evaluated each stem cell's viral burst sizes as an additional means of assessing each stem cell carrier's permissiveness (Figure 1C,D). The consideration of viral burst size remains an important facet of oncolytic delivery, as a carrier's capability to produce sufficient number of viral progeny at its target may determine its successful application. However, undue and premature toxicity to the carrier represents a substantial concern when choosing an ideal stem cell carrier for oncolytic delivery. An ideal carrier would support high levels of viral replication and progeny production, with minimal collateral damage to itself.

Infection of MSCs and NSCs showed a dose-dependent increase in viral burst size (0.1−100 IU) (Figure 1D). NSCs had significantly greater levels of viral progeny at 1 MOI (NSC, 10960000 ± 1784000 IU; MSC, 1318000 ± 105900 IU) and 10 MOI (NSC, 93280000 ± 20730000 IU; MSC, 15540000 ± 1716000 IU). Crystal violet studies conducted alongside viral burst titrations (7 days postinfection) showed that at 100 and 10 IU CRAd-S-pk7 elicited 100% toxicity in MSCs, and partial toxicity at 1 IU CRAd-S-pk7 elicited complete cell killing in NSCs at 100 IU and partial cell killing at 10 IU (Figure 1C).

Migratory Characteristics of NSCs and MSCs toward Malignant Glioma. In order to compare the *in vitro* homing ability of MSCs and NSCs toward glioma, we studied their migration in response to conditioned media from two primary GBM specimens (GBM1 and GBM2) and six human glioma cells lines (U118MG, U87MG, N10, U251MG, A172 and U373MG) (Figure 2). To detect and quantify the total number of cells migrating by fluorescent microscopy, MSCs and NSCs were transduced with lentiviral constructs to generate stable clones that expressed the red fluorescent protein, mCherry.

As illustrated in Supplementary Figure 1A in the Supporting Information, both MSCs and NSCs demonstrated substantial migration in response to the glioma-conditioned medium. A quantitative analysis (Figure 2A) indicated that MSCs exhibited greater nonspecific migratory activity, as shown by their higher level of migration in the negative control group (serum-free medium (SF)) (NSC, 0.9167 ± 0.3632; MSC, 28.83 ± 0.6509)

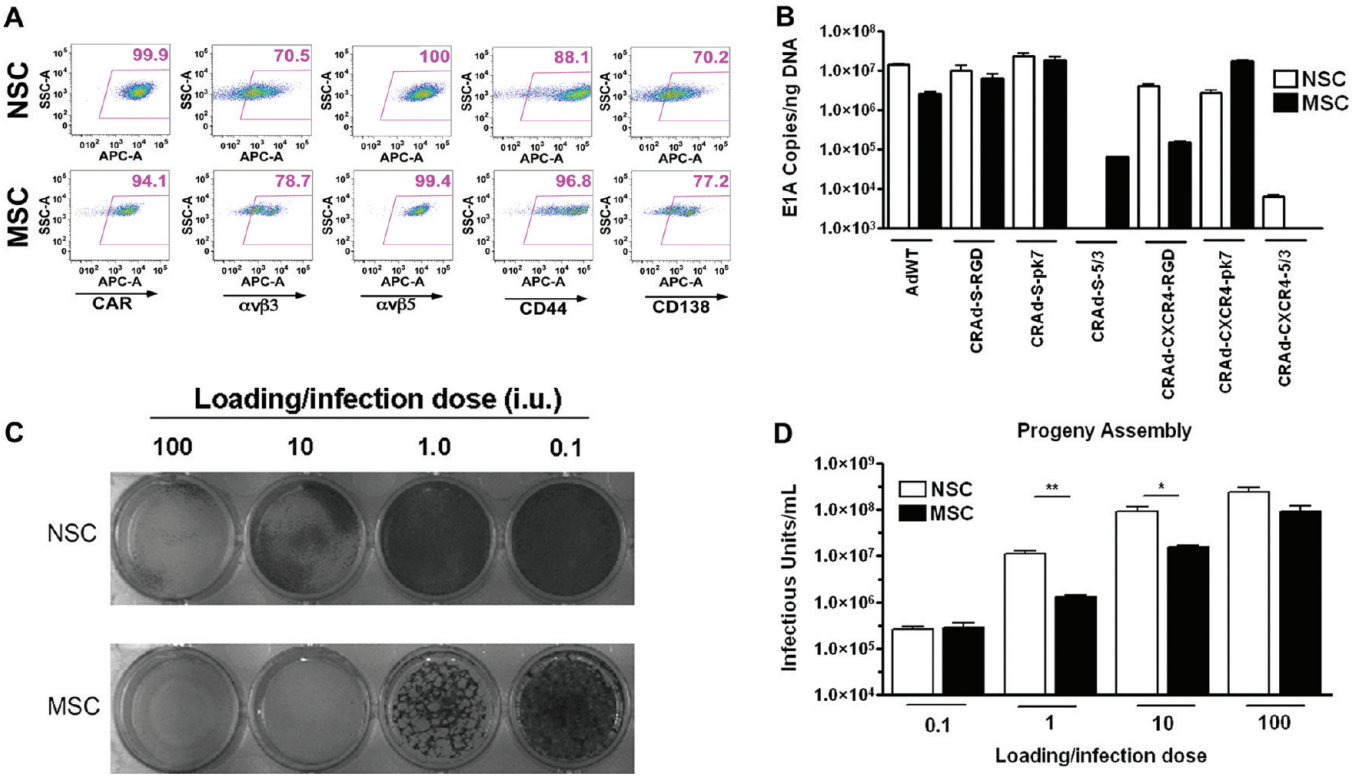

Figure 1. Permissiveness of MSC and NSC for CRAd replication. (A) NSC and MSC were stained to detect the levels of Ad-targeted surface receptors. Numbers in top right corners of each dot plot represent the percentage of positive cells. Gates were drawn using an isotype control sample. *y*-Axis, SSC; *x*-axis, FITC-A. (B) Quantitative PCR detection of viral replication. NSC and MSC were infected with 1 IU of each vector. Seven days postinfection, the degree of viral genome amplification was assessed by measuring the number of viral E1A DNA copies/ng DNA. Bars represent mean of 3 experiments ± standard error (SE). (C) CRAd-S-pk7 cytotoxicity in NSC and MSC. NSC or MSC were infected with CRAd-S-pk7 virus at the indicated iu and stained with crystal violet solution 7 days later. (D) Titration of infectious progeny assembly in NSC and MSC. Studies were conducted alongside crystal violet cytotoxicity studies. MSC were infected with CRAd-S-pk7 at the indicated MOI, and the number of infectious viral progeny was titrated 7 days later. ***, *P*-value <0.001; **, *P*-value <0.01; *, *P*-value <0.05.

(Supplementary Figure 1B in the Supporting Information). We evaluated the migration of MSCs and NSCs as a ratio (represented as the number of cells that migrate in response to a certain conditioned medium/number of cells that migrate in response to SF medium) that can be interpreted as a stem cell carrier's "specific migration". Using this data representation, NSCs demonstrated a greater specific migration in response to GBM1 (NSC, 6.737 ± 1.500; MSC, 1.688 ± 0.07220), GBM2 (NSC, 11.20 ± 0.5350; MSC, 1.889 ± 0.1002), U118 (NSC, 8.408 ± 0.6279; MSC, 1.665 ± 0.06889), N10 (NSC, 5.9433 ± 1.1951; MSC, 1.5319 ± 0.2206), U251 (NSC, 3.641509 ± 0.6623; MSC, 1.2340 ± 0.3576) and U373 (NSC, 5.0188 ± 0.5435; MSC, 2.0425 ± 0.4661) conditioned medium (Figure 2A).

We next evaluated the tumor specific stem cell tracking efficacy by using *in vivo* bioluminescence imaging (BLI). Stem cell lines stably expressing firefly luciferase (SC-Fluc) were first established by using a lentiviral vector. These stem cells (5×10^5) were stereotactically implanted into the brain of mice in the hemisphere contralateral to established U87 xenograft tumors; cell distribution and signal intensity were then assessed in the living animals. The use of BLI for detection of spatial distribution of transplanted stem cells was validated by detecting emitted photons. A focal spot of bioluminescence was observed at the site of injection at 24 h postimplantation (Figure 2B). NSC-mCherry-Fluc and MSC-mCherry-Fluc cells were implanted in the left hemisphere of the nude mouse brain bearing U87 glioma xenograft tumor in the right hemisphere (Figure 2B). As a control, the SC-Fluc cells were implanted in the animal without any established xenograft tumor (Figure 2B-a,d,g,j). Both of the transplanted SC-Fluc crossed the midline and migrated to contralateral hemisphere in the animal brain with the established xenograft tumor within 24 h postimplantation. After 48 h postimplantation, the BLI signal intensity in both stem cell lines decreased significantly. This is likely due to implanted stem cells death as we were unable to histologically detect any viable stem cells within 10−14 days postimplantation (data not shown). Taken together, these findings indicate that both stem cell types are capable of robust migration in response to proliferating glioma; however, NSCs demonstrate a more tumor specific migration. Figure 2C shows representative immunofluorescent analysis of the section of the animal brain from Figure 2B, showing migrated stem cells in the tumor foci contralateral to the original implanted site.

***In Vitro* Delivery and Glioma Stem Cell Toxicity Mediated by MSC and NSC Carriers.** A suitable carrier must successfully usher its therapeutic payload to the tissue of interest. For oncolytic virotherapy, this means that the stem cell must migrate toward the glioma tissue, support viral replication and release viral particles that are capable of subsequently infecting the target tumor cells. Having already assessed the permissiveness of each stem cell carrier and having characterized their migration, we next sought to assess each carrier's ability to migrate when loaded with a different iu, and at the same time to evaluate their ability to

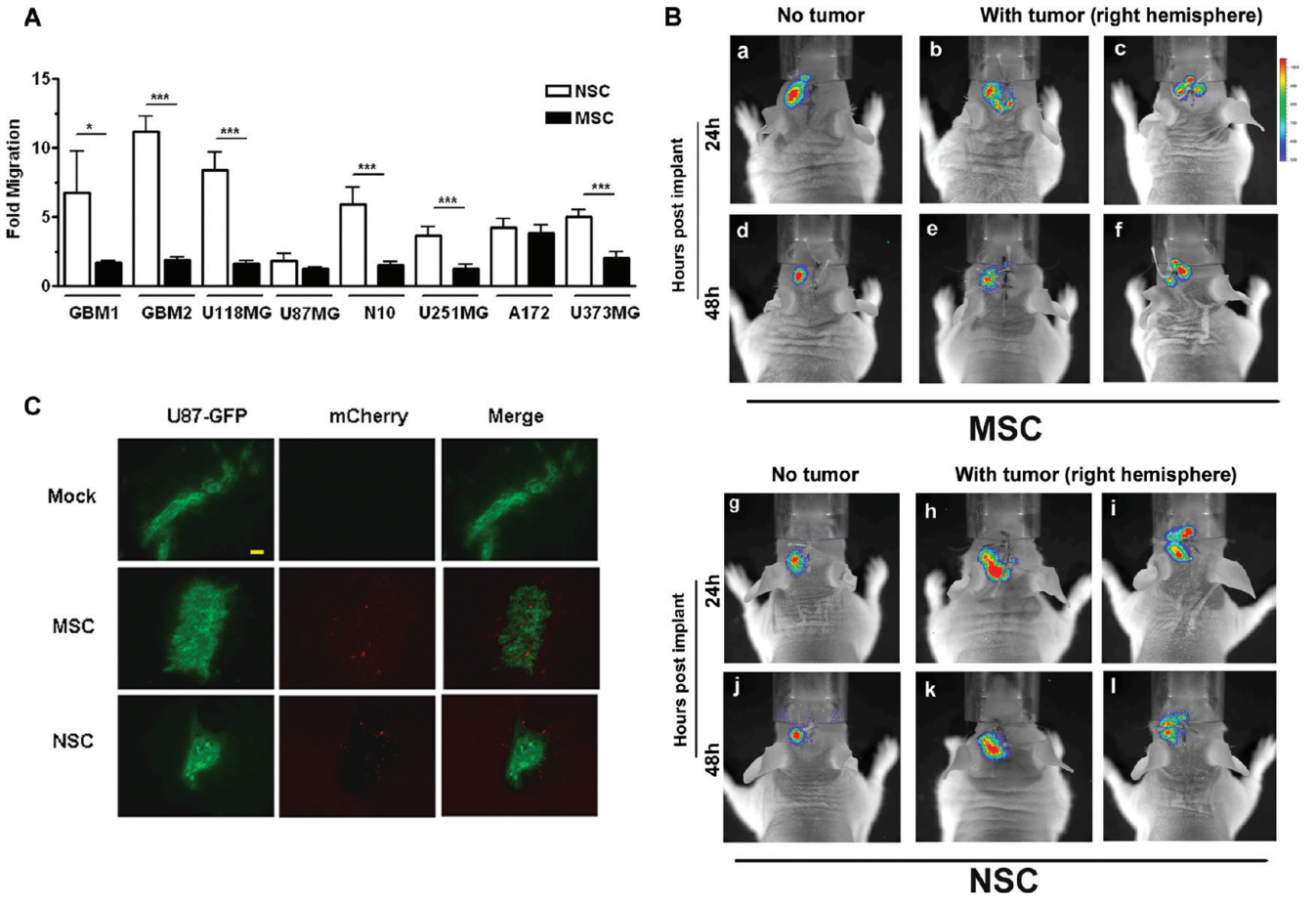

Figure 2. Characterization of MSC and NSC migration in response to human glioma. Migration was studied by using an *in vitro* fluoroblock migration chamber. Conditioned media was generated by culturing each cell type shown in serum-free MEM for twenty-four hours. Migration of each cell type was assessed twenty-four hours after stem cells were plated in the top well of the migration chamber. (A) Specific migration of NSC and MSC toward human glioma. Data obtained in Supplementary Figure 1A in the Supporting Information was used to assess preferential migration (calculated as the number of cells migrating toward glioma-conditioned medium/number of cells migrating in negative control group (SF-MEM). Bar graphs represent mean fold migration ± SE. ***, *P*-value <0.001; **, *P*-value <0.01; *, *P*-value <0.05. (B) *In vivo* tumor tropic migration of MSC and NSC. Bioluminescent imaging of mice after intracranial injection of NSC-Rluc and MSC-Rluc into the left hemisphere of the mice with 7 days postimplanted U87 xenograft tumor (b, c, e, f, h, i, k, l) or mice with no tumor (a, d, g, j). Gradual disappearance of photon emission during 2 days after injection on the injection sites noted. No (for NSC; g, j) or minimal migration (for MSC; a, d) is observed in group with no tumor. (C) Evidence of loaded NSC and MSC tumor-tropic migration *in vivo*. Nude mice received intracranial injections of GFP-expressing U87 cells. Five days later, mice then received injections of PBS (Mock), MSC (mCherry labeled), and NSC (mCherry labeled) in the contralateral hemisphere. Seven days postimplantation of stem cells, animals were sacrificed and animals' brains were subjected to immunohistochemical analysis; bar, 100 μm.

release infectious particles capable of mediating a toxic effect in human glioma cells when loading with different iu of virus.

Malignant glioma cells have been shown to form spheroids in cell cultures; this is a well-documented occurrence for U87 cells when cultured in growth factor-supplemented serum-free media (Figure 3A), and also a characteristic trait of neural and glioma stem cells.[25] These spheroids recapitulate the pathology of malignant glioma *in vivo*;[25] therefore, studying the inhibition of tumor spheroid formation *in vitro* has evolved as an intriguing area of cancer investigations. The number of glioma spheroids formed in each well was quantified nine days after the infected stem cells were plated in the top region of the migration chamber. At all iu, there existed significantly fewer spheroids in the NSC experimental groups than the MSC groups (Figure 3B). A titration of the number of infectious viral particles in the bottom chamber (where U87 spheroids reside) 9 days after plating confirmed that the toxicity observed was due to the release of infectious viral particles. At this time point (9 days), NSCs showed a significantly higher level of progeny release than MSCs at 1 IU (NSC, 1556000 ± 73490 IU; MSC, 872200 ± 118300) and at 100 IU (NSC, 134100000 ± 17990000; MSC, 79500000 ± 5235000) (Supplementary Figure 1A in the Supporting Information).

In order to establish optimal conditions for *in vivo* delivery, we next studied the replication kinetics of the CRAd-S-pk7 virus in the carrier cells at the loading dose of 10 IU/cell. As shown in Figure 3C, the intracellular and released viral progeny reached maximum levels at day 3 postinfection for both types of stem cells. NSCs had a significantly greater number of intracellular CRAd-S-pk7 viral progeny at 1 and 2 days postinfection as compared to MSCs (for day 1, NSC 21420000 ± 3450652, MSC 201600 ± 112697; and for day 2, for NSC 78120000 ± 15170000, MSC 2520000 ± 996117). The progeny released from NSCs at 3 days postinfection was about 1.7 log higher than the progeny released by the infected MSCs (NSC 4254167 ± 2265843,

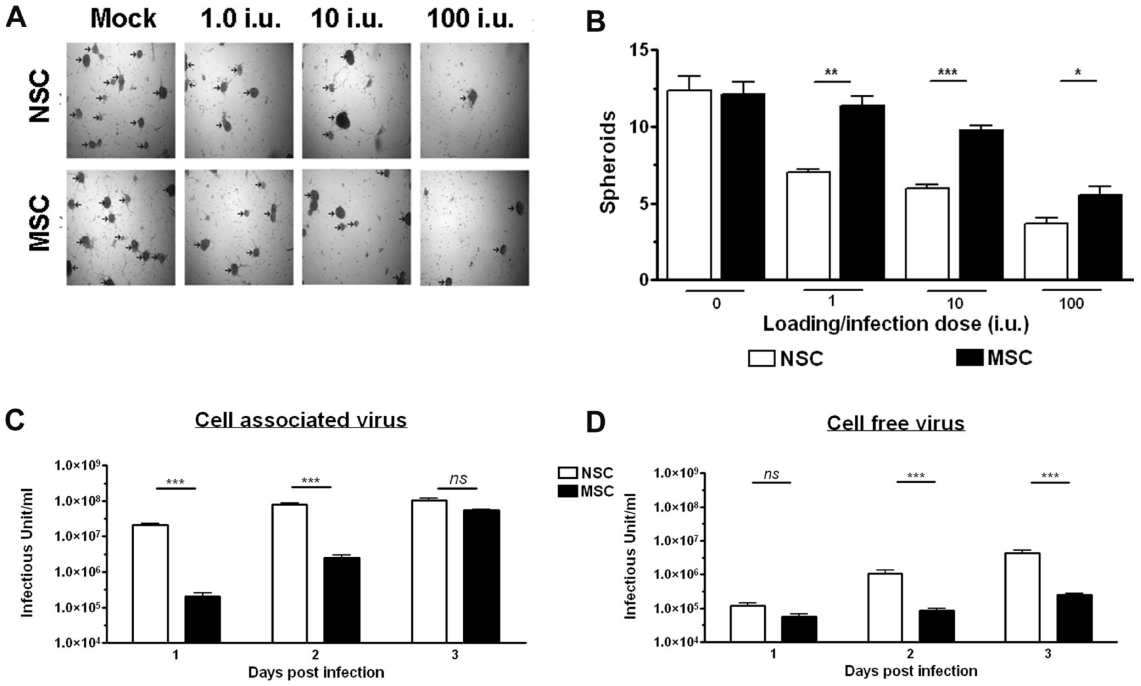

Figure 3. *In vitro* analysis of stem cell loading capacity and glioma toxicity. As in Figure 2, this study employed an *in vitro* Matrigel migration chamber. U87MG cells were cultured for 48 h in SF-MEM supplemented with b-FGF and EGF to generate spheroid colonies, and to serve as an attractant for stem cell migration. After this 48 h culturing period, stem cells were infected with different iu of CRAd-S-pk7 and subsequently plated in the top wells of the migration chamber. (A) Images were taken nine days after infected stem cells were plated in the top well of the migration chamber (original objective, 4×). (B) Inhibition of glioma spheroid formation by stem cell-mediated release of infectious CRAd-S-pk7. The ability of NSC and MSC to release CRAd-S-pk7 and mediate a toxic effect in glioma cells was quantified by counting the number of glioma spheroids (indicated with arrowhead in Figure 3A) formed in the bottom of the migration chamber. Quantification and analysis of spheroid formation (as observed in 3A) mediated by each stem cell when loaded with different iu of CRAd-S-pk7. There were four wells per experimental condition, and three random field views were captured per well. Bar graphs represent mean spheroid number per field view ± SE. (C, D) The replicative capacity of CRAd-S-pk7 virus in stem cells was measured by the titer assay. Media and the cell pellets were separated from the infected well. The total viral progeny in the cell pellets (cell associated) (C) and the progeny released by the infected stem cells over time were measured by the titer assay. Data is presented as the mean infectious units/mL/well ± SE. ***, *P*-value <0.001; **, *P*-value <0.01; *, *P*-value <0.05.

MSC 250000 ± 50000). In conclusion, NSCs permit a more rapid release of infectious viral particles than MSCs (Figure 3D), such that the formation of spheroids is prevented at earlier time points and thus fewer spheroids exist at the time of quantification.

Effect of Oncolytic Virus Loading on the Tumor Tropic Migratory Property of Stem Cells. The carrier's ability to host a viral vector and permit its amplification along with its ability to migrate specifically toward a tumor focus does not necessarily entail the ability to effectively accomplish both tasks at once. Clinical efficacy demands a carrier capable of loading with a viral vector, active migration to tumor microfoci with and subsequent amplification and distribution of its payload. We thus sought to evaluate the carrier's ability to robustly and specifically migrate when loaded with different iu of virus. To do this, we utilized the same migration apparatus employed in the previous section. In the bottom chamber, U87 cells were plated in growth factor-supplemented SF-MEM, thus serving as an attractant for stem cell migration.

Surprisingly, we observed a significant improvement in the tumor-tropic migration of the NSCs after loading them with the oncolytic virus regardless of the loading doses at 24 h postincubation (Figure 4A, $*p < 0.05$ compared to uninfected control). This glioma specific migration was 3−4 times higher by the NSCs as compared to the MSCs in both infected and uninfected population.

Having already shown that MSCs and NSCs are capable of delivering CRAds when injected into a location distant from the tumor injection site,[7,23] we wished to observe and compare the presence of MSCs and NSCs when injected directly into the established intracranial glioma. To observe the presence of loaded stem cells *in vivo*, we utilized mCherry-expressing NSCs and MSCs and GFP-expressing U87MG cells. A total of 54 mice received injections of U87MG cells. One week later, mice were injected with loaded or nonloaded NSCs and MSCs, using the same injection site used for U87MG cells. The presence of loaded and nonloaded MSCs and NSCs in tumor tissues was detected at different time points and recorded (summarized in Table 1). For each group, 3 mice were sacrificed and analyzed at each time point (6 days, 9 days, 12 days after second injection) to detect the presence of fluorescently labeled stem cells. No red fluorescent protein (mCherry) was detected in the control groups (Mock, CRAd-S-pk7). We did not observe the presence of any stem cells in the absence of a tumor mass. The presence of stem cells was always observed within the tumor mass or within close proximity to the tumor. We were able to detect MSCs (nonloaded) only at the first time point of analysis (6 days after injection) in 2 out of the 3 tumor-bearing mice. Similarly, MSCs loaded with virus (MSC + V) were detectable only 6 days after injection in 2 out of 3 tumor-bearing mice. We were able to detect NSCs (nonloaded) at all time points after injection, and NSCs loaded with virus (NSC + V) could be detected up to nine days after injection. In some instances, CRAd-S-pk7-loaded NSCs were detected at a

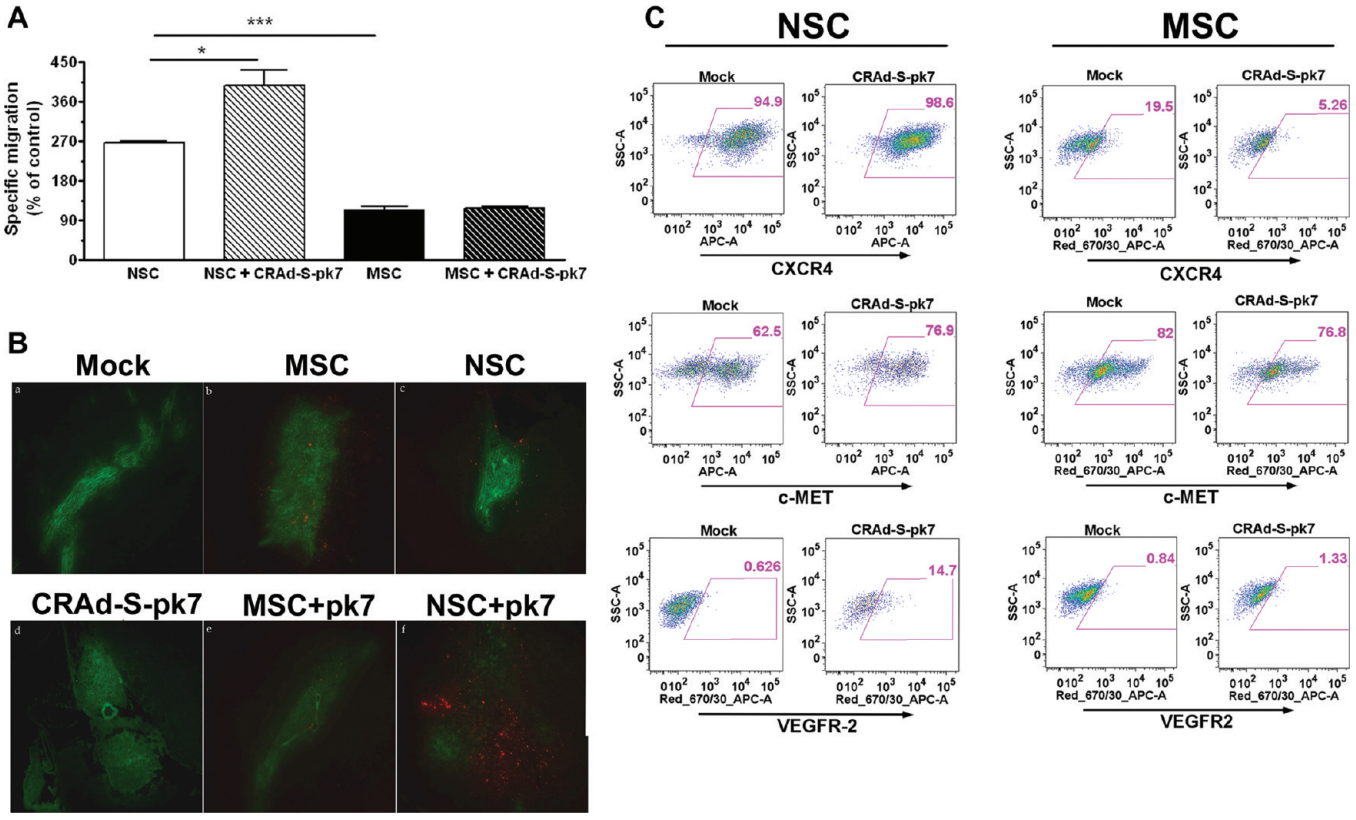

Figure 4. Effects of oncolytic virus loading in the stem cells' tumor-tropic migratory properties. (A) Tumor-tropic migration of CRAd-S-pk7 loaded stem cell in response to U87 cells 24 h after coculture in the Transwell plate. All conditions were done in quadruplicate and repeated in two separate experiments. CRAd-S-pk7 significantly enhanced the *in vitro* tumor-tropic migration of NSCs. $^{*}P < 0.05$, $^{**}P < 0.0005$ significant compare to uninfected control and uninfected MSC. (B) Evidence of loaded NSC and MSC tumor-tropic migration *in vivo*. Nude mice received intracranial injections of GFP-expressing U87MG cells. Five days later, mice received injections of PBS (Mock), MSC (nonloaded), NSC (nonloaded), CRAd-S-pk7, CRAd-S-pk7-loaded MSC (MSC + V), or CRAd-S-pk7-loaded NSC (NSC + V) in the contralateral hemisphere. Injections were performed using the same burr hole used to inject U87MG cells. Images were captured using an inverted fluorescent microscope. The presence of stem cells was detected by the expression of the red fluorescent protein, mCherry; bar 100 μm. (C) Analysis of expression of chemoattractant receptors MET, CXCR4 and VGEFR2 expression postloading with 50 IU of CRAd-S-pk7 virus per stem cells by FACS analysis 48 h postinfection.

much higher frequency as compared to MSCs or their non-infected counterparts (Figure 4B). From this data, we conclude that the tumor tropic migratory property of NSCs is much more robust than that of the MSCs' and that oncolytic virus loading enhances the migratory capacity of NSCs in both *in vitro* and *in vivo* settings. Moreover, *in vivo* NSCs are more resistant to oncolytic virus mediated cell killing and persist longer in the tumor compared to MSCs.

Numerous cytokines, growth factors, and their receptors have been implicated in the tumor homing property of NSCs. Based on this, we next investigated the possible molecular mechanisms behind the CRAd-S-pk7 mediated enhancement of NSCs' tumor-tropic migration by examining the three most well documented chemoattractant receptors reported to regulate stem cell motility. We observed about 14−15% upregulation of the c-Met and the VEGFR2 receptors in the loaded NSCs as compared to MSCs or their noninfected counterparts. This data indicates that loading oncolytic virus into NSCs increases the chemoattractant receptors c-Met and VEGF-R2 expression and enhances their tumor tropic migratory ability both *in vitro* and *in vivo* (Figure 4C).

Immunological Consequence of Oncolytic Adenovirus Loading into the Stem Cells. It has been well documented that most vectors for gene therapy provoke a strong innate immune response upon infection. In order to successfully deliver a therapeutic payload into the disseminated tumor burden, a cell carrier must protect its cargo from the host immune system. The initial innate response of the cell carrier against its viral load will

Table 1. Summary of Fluorescent Microscope Observations[a]

	day 6		day 9		day 12	
conditions	GFP+	RFP+	GFP+	RFP+	GFP+	RFP+
Mock	3/3	0/3	2/3	0/2	3/3	0/3
MSC	3/3	2/3	3/3	0/3	3/3	0/3
NSC	3/3	3/3	2/3	2/2	2/3	2/2
CRAd-S-pk7	3/3	0/3	3/3	0/3	3/3	0/3
MSC + V	3/3	2/3	2/3	0/2	2/3	0/2
NSC + V	3/3	2/3	3/3	2/3	1/3	0/1

[a] There were a total of three mice per group for each time point. Columns are organized according to the time of observation after each type of injection. Experimental groups are organized in rows. The GFP+ columns indicate the number of mice per group that harbored tumor masses identifiable by GFP signal. The RFP+ columns indicate how many of the GFP-positive animals of that group were also positive for red fluorescent protein (RFP+ animals/GFP+ animals).

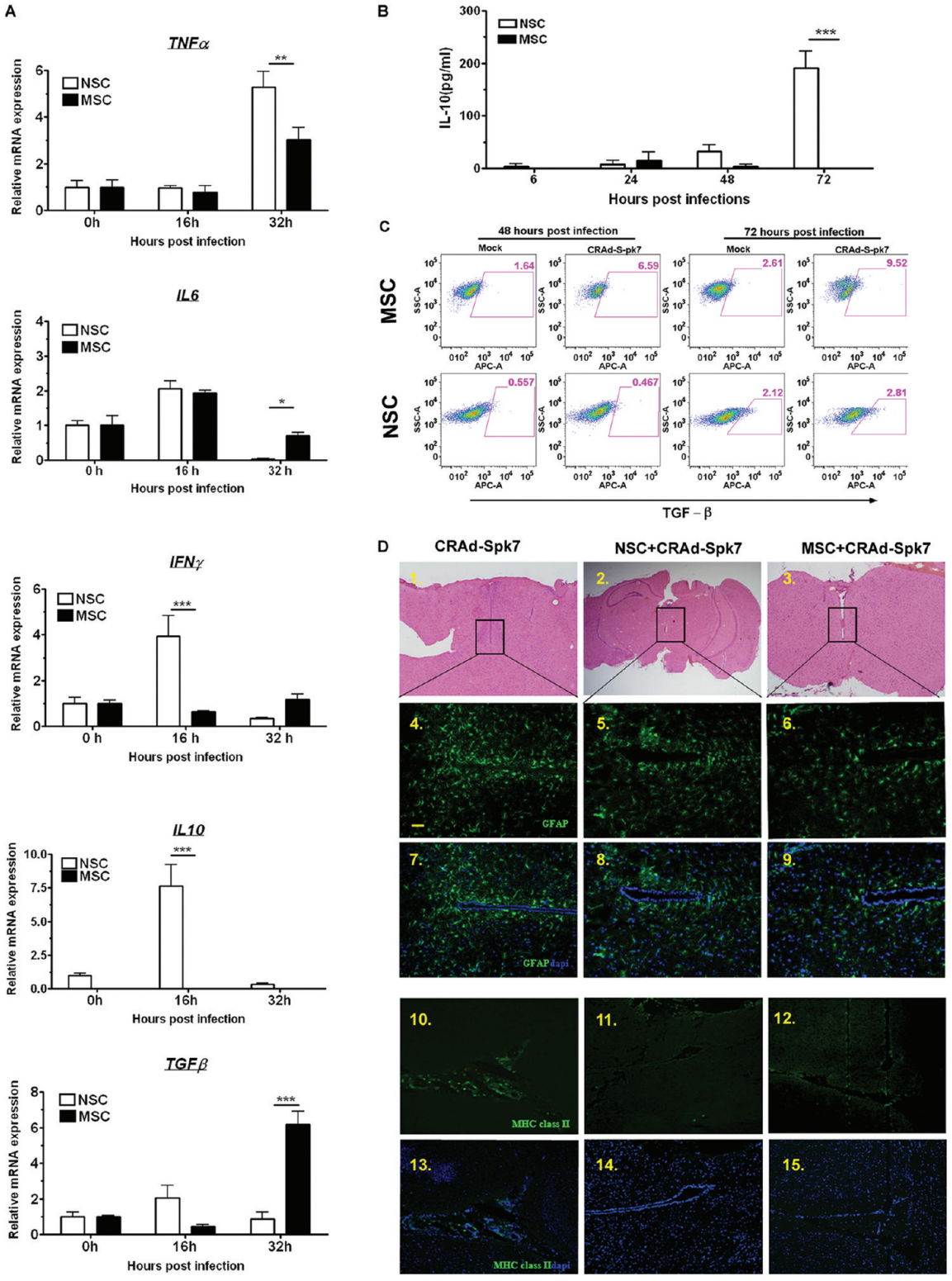

Figure 5. Immunological consequences of oncolytic adenovirus loading into stem cells. (A) Analysis of cytokine expression postinfection with 10 IU of CRAd-S-pk7 virus per stem cells by qRT-PCR. Levels of expression were expressed relative to uninfected control for each stem cell line at 0 h; $^{*}P < 0.05$, $^{**}P < 0.005$, $^{***}P < 0.0005$ significant. (B) Analysis of IL-10 cytokine expression in stem cells infected with CRAd-S-pk7 (10 IU/cell). Supernatant from the infected stem cell culture was harvested at 6, 24, 48 and 72 h postinfection, and IL-10 expression was measured by ELISA; $^{***}p < 0.0005$. (C) Analysis of TGF-β positive stem cells by FACS at 48 and 72 h postinfection with CRAd-S-pk7 (10 IU/cell). (D) Histological features of brains from mice injected with CRAd-S-pk7 virus alone (2.5×10^7 iu/ injection) or virus loaded into stem cells (5×10^5 cells loaded with 50 IU of CRAd-S-pk7 per NSCs) harvested at day 14 postinjection. (1−3) Image of H&E staining assessing neuronal toxicity postinjection. Representative image of sections of the same animal brain as H&E sections stained with antiglial fibrillary acidic protein (GFAP) (4−9) and anti-mouse MHC class II antibody (10−15); bar, 50 μm.

dx.doi.org/10.1021/mp200161f |*Mol. Pharmaceutics* 2011, 8, 1559–1572

dictate the force of the host immune response to the therapeutic cargo by encouraging or discouraging attack via secreted and cell bound signaling. Based on this, we examined the innate immune modulators involved in the response to adenovirus infection by qRT-PCR in stem cells. Adenovirus infection induces numerous genes associated with the innate immune responses in the target cells including IL-6, tumor necrosis factor α (TNF-α), interferon γ, monocytes chemoattractant protein 1 (MCP-1) and RANTES within a few hours of infection.[26] As shown in Figure 5A, proinflammatory cytokines such as IL-6 and TNF-α were significantly upregulated within 16 and 32 h, respectively, in response to CRAd-S-pk7 loading/infection in both of the stem cells. The IL-6 transcript level in infected MSCs was significantly elevated at 32 h postinfection (Figure 5A, $^{**}p < 0.05$ compared to NSC); the IFNγ and the TNFα transcript levels were significantly elevated in the NSC postinfection (Figure 5A, $^{***}p < 0.0005$ and $^{**}p < 0.005$ respectively as compared to MSC). We also observed, very surprisingly, that the adenovirus also increased the expression of the anti-inflammatory gene IL-10 about 10-fold at 16 h after loading in the NSCs and elevated TGF-β transcript in the loaded MSCs at 32 h postinfection (Figure 5A). IL-10 expression at the protein level was next evaluated by ELISA assay and also showed elevated expression in NSCs infected with CRAd-S-pk7 at 72 h postinfection (Figure 5B). FACS analysis of the TGF-β expressing stem cells showed about a 4-fold increase in TGF-β positive MSCs at 48 and 72 h postloading/postinfection with the CRAd-S-pk7 virus (Figure 5C). In summary, these results indicate that loading CRAd-S-pk7 into carrier cell NSCs leads to the expression of both pro- and anti-inflammatory genes.

The host immune response against the therapeutic oncolytic adenovirus is considered one of the major obstacles to the successful application of this approach in clinical settings.[27,28] The immunosuppressive properties of NSCs are well documented in both *in vitro* and *in vivo* animal models.[27−29] Taken together, we hypothesized that loading oncolytic adenovirus into NSCs may reduce the host immune activation in response to the therapeutic virus. To test this hypothesis, we injected naked CRAd-S-pk7 virus or virus loaded into human NSCs in the brain of nude mice; animals were sacrificed 14 days after the treatment to evaluate the immune activation. Assessment of neuronal damage was first undertaken in sections stained with hematoxylin-eosin (H&E) 14 days following various treatments (Figure 5D, 1−3). We evaluated the extent of neuroinflammation in the different treatment groups by immunohistochemical analysis of glial fibrillary acidic protein (GFAP) (Figure 5D, 4−9), major histocompatibility complex (MHC) class II (Figure 5D, 10−15) and observed that the animals that received oncolytic adenovirus alone had a higher number of GFAP and MHC class II immunoreactive cells at the injection site as compared to the animals that received oncolytic virus loaded into different stem cells. Therefore, the delivery of oncolytic virus to the brain loaded with both MSCs and NSCs reduced the activation of the resident microglia and astrocytes in response to adenoviral vector.

Oncolytic Virus Loaded NSCs Prolong Survival of Mice with Orthotopic Glioblastoma. To determine whether CRAd-S-pk7 loaded stem cell are effective against glioma *in vivo*, U87 (2.5×10^5) cells were implanted into the right hemisphere of athymic nude mice. Five days postimplantation of the glioma xenograft, we administered a single intratumoral injection of CRAd-S-pk7 (2.5×10^7 iu) loaded into stem cells (2.5×10^7 iu = loading dose 50 IU/cell of the oncolytic virus loaded into 5×10^5 of carrier cells), and the animals were monitored for survival analysis.

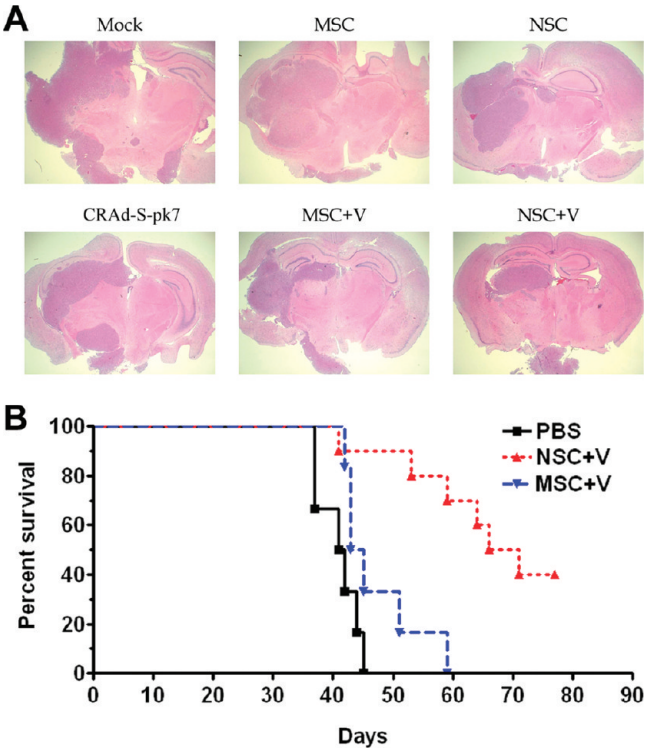

Figure 6. Oncolytic virus loaded NSCs inhibit xenograft growth and prolong survival of mice with orthotopic glioblastoma. (A) Three animals from different groups in the experiment described below (6B) were sacrificed 30 days post therapy and their brains were subject to H&E analysis to assess the tumor burden. H&E staining of representative animals' brains were shown (original objective, 40×). (B) Both stem cell lines were incubated with the oncolytic adenovirus (50 IU/cells) for 2 h in the room temperature, washed 3 times with PBS, and resuspended in PBS (5×10^5 stem cells in 2.5 μL/mouse) before intratumoral injection. 5×10^5 U87 cells were injected stereotactically into the right hemisphere of the brain of 9 to 12 week old *nu/nu* mice followed by intratumoral (IT) injection of CRAd-S-pk7 loaded into stem cells 5 days post tumor implantation. The median survival for animals injected with PBS was 41.4 days, with MSC loaded CRAd-S-pk7 it was 44 days (log-rank, $P = 0.075$), and with NSC loaded CRAd-S-pk7 it was 68.5 days, $n = 7$ ($P < 0.002$ vs MSC). Data are presented from two independent experiments.

Three animals from each group were sacrificed 30 days post-therapy, and diseased brains were subjected to H&E analysis to evaluate the tumor burdens. Figure 6A shows the representative animal brains from this experiment. As a control, we intratumorally injected equal volumes of PBS and the same number of NSCs without the therapeutic virus, and the survival was very similar to PBS treated control group (data not shown). The median survival for the group treated with MSC loaded CRAd-S-pk7 was 44 days as compared to 68.5 days in the NSC+CRAd-S-pk7 group ($p < 0.002$). These results indicate that CRAd-S-pk7-loaded NSCs delivered oncolytic adenovirus to malignant glioma *in vivo* resulting in a significant inhibition of tumor growth with a simultaneous increase in median survival of the treated animals.

DISCUSSION

Carrier based oncolytic virotherapy holds great promise as an emerging treatment modality for highly aggressive and therapy resistant malignancies. In theory, it can combine the potent and specific antitumor effects of designer viruses with the robust and

relatively benign distribution capacity of carrier cells. Diffusely infiltrative, highly aggressive and refractory to most conventional therapies, glioblastoma represents a paradigm for the type of cancer that could benefit from such a therapeutic approach. In this study we sought to evaluate the relative efficacy of two promising cell carrier systems, neural and mesenchymal stem cells. We first established the optimal oncolytic virus to be employed as the therapeutic payload for subsequent experiments. Both cell lines were found to prominently express receptors necessary for entry by a variety of engineered oncolytic adenoviruses. Permissiveness to a panel of viruses was next explored (Figure 1B), and the virus CRAd-S-pk7 was selected due to its robust and comparable expression by both cell lines of interest.

We next evaluated each stem cell's viral burst size as an additional means of assessing permissiveness. Magnitude of viral burst size may serve as an important surrogate marker for ultimate therapeutic efficacy, an inability to produce a significant burst may limit individual carrier's area of effect *in vivo*. In this aspect, NSCs were much more effective in supporting CRAd-S-pk7 viral replication as compared to MSCs (Figures 1D and 3C). Most importantly, total progeny released from infected NSCs was about a log higher than that released by MSCs at 3 days postloading (Figure 3D). The molecular mechanisms behind the enhanced ability of NSCs to support adenoviral replication remain to be investigated. It may be due to the fact that the NSC cell line used in this study is an immortalized cell line providing for a greater rate of doubling and improved cellular stability, which possibly leads to higher levels of viral replication. Unwanted and premature toxicity to the carrier cells further represents a major concern when choosing an ideal stem cell carrier for oncolytic virus delivery. Carrier toxicity is an inevitable byproduct of the site-specific amplification of the therapeutic vector, but counterproductive for the long-term survival and tumor-specific homing of the carrier cells. Premature lysis of cell carriers will reduce the dose of the therapeutic payload at the target sites and frivolously distribute virus to normal parenchyma. An ideal carrier would support high levels of viral replication and progeny production while minimizing collateral damage to the carrier. With that in mind, our *in vitro* and *in vivo* experiments revealed that MSCs were more susceptible to CRAd-S-pk7 mediated killing as compared to NSCs (Figure 1C and Table 1). The successful clinical translation of such delivery system will require additional modifications that will reduce the lytic activity of the therapeutic virus selectively in the carrier cells in order to prolong their survival and allow them to home to disseminated tumor burdens more efficiently.

The ability of stem cells to migrate to tumors is central to their utility as carriers of therapeutic, anti-neoplastic agents. Our results show that even though the migratory capacity of MSCs toward primary GBM samples was statistically similar to that of NSCs (Supplementary Figure 1A in the Supporting Information), MSCs showed a greater nonspecific migration both *in vitro* and *in vivo* (Supplementary Figure 1 in the Supporting Information and Figure 2B-a). Numerous cytokines, growth factors and receptors have been implicated in the tumor homing property of NSCs, including SCF/c-Kit,[30] SDF1/CXCR4,[31] HGF/c-Met,[32] VEGF/VEGFR,[33] MCP-1/CCR2.[34] We have shown that *in vitro* tumor-tropic migratory properties of oncolytic adenovirus loaded NSC can be inhibited by the blocking antibody against the chemokine receptors such as CXCR4 and VEGFR2.[35] Based on this concept, we examined the expression of various chemoattractant receptors and observed that the CXCR4 expression was much higher in the NSCs, whereas MSCs expressed a high level of c-MET receptors as compared to NSCs. Based on published reports, we speculate that high levels of CXCR4 expression may be responsible for the NSCs' admirable migratory specificity toward human glioma.[36] Even though the contribution of these chemoattractant receptors to the tumor specific migratory properties of the stem cells is well documented, further examination remains into their involvement in the migratory properties of the stem cell lines used in our study.

In order to be effective in the clinical setting, stem cell-based cell carriers must maintain their natural tropism for tumor cells after loading with the oncolytic virus. Our data indicate that CRAd-S-pk7 loading significantly enhances the tumor specific migratory ability of NSCs both *in vitro* and *in vivo* (Figure 4A,B). This is potentially due to the fact that oncolytic virus enhanced the expression of all three chemoattractant receptors examined at 48 h postinfection (Figure 4C). In contrast, the *in vitro* migratory capacity of MSCs was not affected by the loading of the oncolytic virus (Figure 4A). We further observed the downregulation of the chemoattractant receptors CXCR4 and c-MET following CRAd-S-pk7 infection in the MSC (Figure 4C). The molecular mechanisms regarding the CRAd-S-pk7 mediated regulation of these chemoattractant receptors remains to be elucidated. We suggest that the differing expression patterns of these receptors are regulated in part by the diverse innate immune responses of NSCs and MSCs after CRAd-S-pk7 infection. For example, it has been reported that cytokines such as IL-10 can upregulate surface CXCR4 expression in NSCs.[37] We also observed that CRAd-S-pk7 induced a high level of IL-10 expression in the NSCs within 48 h of infection (Figure 5A,B). Moreover, the induction of these chemoattractant receptors was very rapid after CRAd-S-pk7 exposure, which led us to speculate that their upregulation may be a component of the NSC's antiviral innate immune response itself. Additional experiments aimed at understanding the effects of oncolytic adenovirus loading on stem cell phenotypes, differentiation and migration may serve to expand our view of this phenomenon.

Immunosuppressive properties of stem cells are well documented in the literature.[27,38] Transplanted NSCs were shown to elicit an anti-inflammatory response in the rat experimental autoimmune encephalomyelitis (EAE) model.[39] Extensive *in vitro* studies have demonstrated that MSCs are also nonimmunogenic and immunosuppressive.[40] This is a very attractive characteristic for stem cells as cell carriers given that such qualities will not only allow therapeutic viruses to be hidden from host immunosurveillance but also may suppress local inflammation during virotherapy, thus allowing the OV to replicate and kill tumor cells without any immune restriction. Our laboratory has used bone marrow-derived cotton rat MSCs to deliver oncolytic adenovirus intratumorally in an immunocompetent cotton rat model and observed that OV loaded MSC persist longer in the tumor and the antiviral immune response is significantly inhibited.[41] In this report, we show that both stem cell lines activate innate immune responses within 16 h postloading with the adenovirus. But to our surprise, we also observed induction of immunosuppressive cytokines such as IL10 in NSC and TGF-β expression in MSC as compared to uninfected control (Figure 5A−C). These observations support the use of stem cells as a platform of cell carrier to circumvent the antiviral immune response in the oncolytic virotherapy.

The stem cell derivatives presented in this report have demonstrated inherent tumor-tropic properties in a variety of

animal brain tumor models.[42] The available preclinical data strongly argues in favor of the hypothesis that a stem cell-based delivery system can be clinically effective in the targeted delivery of a therapeutic agent to the disseminated tumor burdens in the brain.[3,4,7,23] Stem cells expressing a variety of anticancer agents have resulted in clinically relevant therapeutic efficacy in several xenograft animal models. Before the transition into clinical trials may be undertaken, an optimal cell carrier system must be clearly and conclusively identified. With this goal in mind, we compared NSCs and MSCs, the most widely used stem cell types for targeting brainstem glioma, as cell carriers for antiglioma oncolytic virotherapy. Due to their origin, we argue that NSCs are more suitable as therapeutic delivery vehicles for brain tumors. Unlike MSCs, NSCs have the inherent capacity to migrate into the host brain without disrupting the normal functions of the target organ, a favorable trait when considering potential treatment related complications. The clinical application of NSCs is however limited due to logistical problems related to their potential immunogenicity and the risk of secondary malignancy associated with the use of an immortalized cell line.[43] An ideal cell delivery system should be stable in the tissue culture or technology must be in place to isolate large quantities of autologous carrier cells from patients. These cells could then be modified to carry the therapeutic payload to targeted sites. Most of the NSC lines used thus far as cell carriers have been immortalized by the induction of an oncogene to provide for stability in cell culture. Despite this, most available NSC lines have been well characterized with favorable preclinical safety profiles and have not been found to result in the formation of tumors in immunodeficient mice for up to 12 months.[19] The transition to human clinical trials, however, presents a vastly different landscape, and thus the safety concern regarding secondary malignancies must not be overlooked.

In contrast, the feasibility of using autologous MSCs as a cell carriers for oncolytic viral therapy is very attractive because it may allow us to avoid discussion of allograft rejection altogether. The use of freshly isolated MSCs is partially limited by the fact that they represent a more heterogeneous cell type, making it harder to predict their behavior and success in delivering oncolytic adenovirus *in vivo*. There is likely much variation in the suitability of MSCs for therapeutic use, depending on the patient's age, current health status, etc.[44] Additionally, at this juncture it is difficult to predict the likelihood that a 63 year old patient with a brain tumor, who has undergone multiple cycles of chemotherapy/radiation, will have sufficient healthy bone marrow cells to be tailored for effective therapy.[44] Additional studies would be needed to classify the suitability of patients' MSCs for therapeutic use based on age, performance status, the chemotherapeutic regimens they have undergone, etc.

There may be some limitations to our study. First, we only used MSCs derived from human bone marrow. There are many different types of MSCs whose use as cell carriers has recently been reported for antiglioma therapy. Future comparison studies must include stem cell types derived from other tissue types. Furthermore, we only used one human glioma cell line to evaluate the migratory and therapeutic potential of different stem cell carrier systems *in vivo*, which may have resulted in a biased outcome due to differences in *in vivo* tumor phenotypes between cell lines. These experiments need to be further evaluated in multiple human glioma cell lines or even with the freshly isolated human glioma specimens. Second, it is not known how the pluripotency and cellular differentiation status of the stem cells are altered upon viral infection. This will be a very important piece of information when selecting the optimal stem cell as a carrier, because differentiation status will likely influence migratory ability. Finally, the *in vivo* tumor-tropic migratory kinetics of these stem cells must be evaluated quantitatively. Real time dynamic determination of carrier cell migration and tumor distribution is essential for optimizing treatments in preclinical models and designing clinical protocols. Bioluminescence imaging is employed in this study as a noninvasive method to track NSCs migration and monitor therapeutic efficacy in animal models. However, due to poor tissue penetration and low spatial resolution, it is extremely difficult to utilize the data generated from this approach to make quantitative conclusions regarding the migratory kinetics of the transplanted stem cells. Moreover, the clinical utility of this imaging modality is limited and impractical for use in patient trials. On the other hand, magnetic resonance imaging (MRI) cellular tracking is a rapidly expanding field included in many studies that have been published during the past decade.[45] Use of more sensitive and clinically relevant techniques such as MRI must be carried out for further careful evaluation of the migratory kinetics of the transplanted NSCs.

In conclusion, our study shows that NSC-based cell carriers have significant advantages as delivery vehicles for oncolytic virotherapy against brain tumors. Our findings suggest that NSC-mediated delivery of CRAd-S-pk7 in an orthotopic glioma model significantly prolong survival of animals compared to control. These findings support the notion that a stem cell-based cell carrier system is a viable approach to the targeted delivery of oncolytic viruses for the treatment of malignant glioma.

■ ASSOCIATED CONTENT

Supporting Information. Figure depicting characterization of MSC and NSC migration in response to human glioma. This information is available free of charge via the Internet at http://pubs.acs.org/.

■ AUTHOR INFORMATION

Corresponding Author

*The Brain Tumor Center, The University of Chicago Pritzker School of Medicine, 5841 South Maryland Ave, MC 3026, Chicago, IL 60637. Tel: (773) 834-4757. Fax: (773) 834-2608. E-mail: mlesniak@surgery.bsd.uchicago.edu.

■ ACKNOWLEDGMENT

We would like to thank Simona M. Ahmed for editing the manuscript, Dingcai Cao and Feifei Liu for statistical analysis. This research was supported by the NCI (R01CA122930, R01CA138587), the National Institute of Neurological Disorders and Stroke (U01NS069997), the American Cancer Society (RSG-07-276-01-MGO) and University of Chicago BSD IRI Pilot Grant.

■ REFERENCES

(1) Deorah, S.; Lynch, C. F.; Sibenaller, Z. A.; Ryken, T. C. Trends in brain cancer incidence and survival in the United States: Surveillance, Epidemiology, and End Results Program, 1973 to 2001. *Neurosurg. Focus* **2006**, *20* (4), E1.

(2) Lesniak, M. S. Novel advances in drug delivery to brain cancer. *Technol. Cancer Res. Treat.* **2005**, *4* (4), 417–28.

(3) Aboody, K. S.; Brown, A.; Rainov, N. G.; Bower, K. A.; Liu, S.; Yang, W.; Small, J. E.; Herrlinger, U.; Ourednik, V.; Black, P. M.; Breakefield, X. O.; Snyder, E. Y. Neural stem cells display extensive tropism for pathology in adult brain: evidence from intracranial gliomas. *Proc. Natl. Acad. Sci. U.S.A.* **2000**, *97* (23), 12846–51.

(4) Benedetti, S.; Pirola, B.; Pollo, B.; Magrassi, L.; Bruzzone, M. G.; Rigamonti, D.; Galli, R.; Selleri, S.; Di Meco, F.; De Fraja, C.; Vescovi, A.; Cattaneo, E.; Finocchiaro, G. Gene therapy of experimental brain tumors using neural progenitor cells. *Nat. Med.* **2000**, *6* (4), 447–50.

(5) Herrlinger, U.; Woiciechowski, C.; Sena-Esteves, M.; Aboody, K. S.; Jacobs, A. H.; Rainov, N. G.; Snyder, E. Y.; Breakefield, X. O. Neural precursor cells for delivery of replication-conditional HSV-1 vectors to intracerebral gliomas. *Mol. Ther.* **2000**, *1* (4), 347–57.

(6) Nakamura, K.; Ito, Y.; Kawano, Y.; Kurozumi, K.; Kobune, M.; Tsuda, H.; Bizen, A.; Honmou, O.; Niitsu, Y.; Hamada, H. Antitumor effect of genetically engineered mesenchymal stem cells in a rat glioma model. *Gene Ther.* **2004**, *11* (14), 1155–64.

(7) Tyler, M. A.; Ulasov, I. V.; Sonabend, A. M.; Nandi, S.; Han, Y.; Marler, S.; Roth, J.; Lesniak, M. S. Neural stem cells target intracranial glioma to deliver an oncolytic adenovirus in vivo. *Gene Ther.* **2009**, *16* (2), 262–78.

(8) Willmon, C.; Harrington, K.; Kottke, T.; Prestwich, R.; Melcher, A.; Vile, R. Cell carriers for oncolytic viruses: Fed Ex for cancer therapy. *Mol. Ther.* **2009**, *17* (10), 1667–76.

(9) Ahmed, A.; Thompson, J.; Emiliusen, L.; Murphy, S.; Beauchamp, R. D.; Suzuki, K.; Alemany, R.; Harrington, K.; Vile, R. G. A conditionally replicating adenovirus targeted to tumor cells through activated RAS/P-MAPK-selective mRNA stabilization. *Nat. Biotechnol.* **2003**, *21* (7), 771–7.

(10) Sonabend, A. M.; Ulasov, I. V.; Han, Y.; Lesniak, M. S. Oncolytic adenoviral therapy for glioblastoma multiforme. *Neurosurg. Focus* **2006**, *20* (4), E19.

(11) Fisher, K. Striking out at disseminated metastases: the systemic delivery of oncolytic viruses. *Curr. Opin. Mol. Ther.* **2006**, *8* (4), 301–13.

(12) Coukos, G.; Makrigiannakis, A.; Kang, E. H.; Caparelli, D.; Benjamin, I.; Kaiser, L. R.; Rubin, S. C.; Albelda, S. M.; Molnar-Kimber, K. L. Use of carrier cells to deliver a replication-selective herpes simplex virus-1 mutant for the intraperitoneal therapy of epithelial ovarian cancer. *Clin. Cancer Res.* **1999**, *5* (6), 1523–37.

(13) Mader, E. K.; Maeyama, Y.; Lin, Y.; Butler, G. W.; Russell, H. M.; Galanis, E.; Russell, S. J.; Dietz, A. B.; Peng, K. W. Mesenchymal stem cell carriers protect oncolytic measles viruses from antibody neutralization in an orthotopic ovarian cancer therapy model. *Clin. Cancer Res.* **2009**, *15* (23), 7246–55.

(14) Ehtesham, M.; Stevenson, C. B.; Thompson, R. C. Stem cell therapies for malignant glioma. *Neurosurg. Focus* **2005**, *19* (3), E5.

(15) Brustle, O.; Spiro, A. C.; Karram, K.; Choudhary, K.; Okabe, S.; McKay, R. D. In vitro-generated neural precursors participate in mammalian brain development. *Proc. Natl. Acad. Sci. U.S.A.* **1997**, *94* (26), 14809–14.

(16) Caplan, A. I. The mesengenic process. *Clin. Plast. Surg.* **1994**, *21* (3), 429–35.

(17) Gregory, C. A.; Ylostalo, J.; Prockop, D. J. Adult bone marrow stem/progenitor cells (MSCs) are preconditioned by microenvironmental "niches" in culture: a two-stage hypothesis for regulation of MSC fate. *Sci. STKE* **2005**, *2005* (294), pe37.

(18) Pittenger, M. F.; Mackay, A. M.; Beck, S. C.; Jaiswal, R. K.; Douglas, R.; Mosca, J. D.; Moorman, M. A.; Simonetti, D. W.; Craig, S.; Marshak, D. R. Multilineage potential of adult human mesenchymal stem cells. *Science* **1999**, *284* (5411), 143–7.

(19) Ahmed, A. U.; Alexiades, N. G.; Lesniak, M. S. The use of neural stem cells in cancer gene therapy: predicting the path to the clinic. *Curr. Opin. Mol. Ther.* **2010**, *12* (5), 546–52.

(20) Shaner, N. C.; Campbell, R. E.; Steinbach, P. A.; Giepmans, B. N.; Palmer, A. E.; Tsien, R. Y. Improved monomeric red, orange and yellow fluorescent proteins derived from Discosoma sp. red fluorescent protein. *Nat. Biotechnol.* **2004**, *22* (12), 1567–72.

(21) Deregowski, V.; Canalis, E. Gene delivery by retroviruses. *Methods Mol. Biol.* **2008**, *455*, 157–62.

(22) Ulasov, I. V.; Zhu, Z. B.; Tyler, M. A.; Han, Y.; Rivera, A. A.; Khramtsov, A.; Curiel, D. T.; Lesniak, M. S. Survivin-driven and fiber-modified oncolytic adenovirus exhibits potent antitumor activity in established intracranial glioma. *Hum. Gene Ther.* **2007**, *18* (7), 589–602.

(23) Sonabend, A. M.; Ulasov, I. V.; Tyler, M. A.; Rivera, A. A.; Mathis, J. M.; Lesniak, M. S. Mesenchymal stem cells effectively deliver an oncolytic adenovirus to intracranial glioma. *Stem Cells* **2008**, *26* (3), 831–41.

(24) Ulasov, I. V.; Rivera, A. A.; Sonabend, A. M.; Rivera, L. B.; Wang, M.; Zhu, Z. B.; Lesniak, M. S. Comparative evaluation of survivin, midkine and CXCR4 promoters for transcriptional targeting of glioma gene therapy. *Cancer Biol. Ther.* **2007**, *6* (5), 679–85.

(25) Yu, S. C.; Ping, Y. F.; Yi, L.; Zhou, Z. H.; Chen, J. H.; Yao, X. H.; Gao, L.; Wang, J. M.; Bian, X. W. Isolation and characterization of cancer stem cells from a human glioblastoma cell line U87. *Cancer Lett.* **2008**, *265* (1), 124–34.

(26) Muruve, D. A. The innate immune response to adenovirus vectors. *Hum. Gene Ther.* **2004**, *15* (12), 1157–66.

(27) Einstein, O.; Ben-Hur, T. The changing face of neural stem cell therapy in neurologic diseases. *Arch. Neurol.* **2008**, *65* (4), 452–6.

(28) Pluchino, S.; Quattrini, A.; Brambilla, E.; Gritti, A.; Salani, G.; Dina, G.; Galli, R.; Del Carro, U.; Amadio, S.; Bergami, A.; Furlan, R.; Comi, G.; Vescovi, A. L.; Martino, G. Injection of adult neurospheres induces recovery in a chronic model of multiple sclerosis. *Nature* **2003**, *422* (6933), 688–94.

(29) Pluchino, S.; Zanotti, L.; Rossi, B.; Brambilla, E.; Ottoboni, L.; Salani, G.; Martinello, M.; Cattalini, A.; Bergami, A.; Furlan, R.; Comi, G.; Constantin, G.; Martino, G. Neurosphere-derived multipotent precursors promote neuroprotection by an immunomodulatory mechanism. *Nature* **2005**, *436* (7048), 266–71.

(30) Sun, L.; Lee, J.; Fine, H. A. Neuronally expressed stem cell factor induces neural stem cell migration to areas of brain injury. *J. Clin. Invest.* **2004**, *113* (9), 1364–74.

(31) Carbajal, K. S.; Schaumburg, C.; Strieter, R.; Kane, J.; Lane, T. E. Migration of engrafted neural stem cells is mediated by CXCL12 signaling through CXCR4 in a viral model of multiple sclerosis. *Proc. Natl. Acad. Sci. U.S.A.* **2010**, *107* (24), 11068–73.

(32) Heese, O.; Disko, A.; Zirkel, D.; Westphal, M.; Lamszus, K. Neural stem cell migration toward gliomas in vitro. *Neuro. Oncol.* **2005**, *7* (4), 476–84.

(33) Schmidt, N. O.; Koeder, D.; Messing, M.; Mueller, F. J.; Aboody, K. S.; Kim, S. U.; Black, P. M.; Carroll, R. S.; Westphal, M.; Lamszus, K. Vascular endothelial growth factor-stimulated cerebral microvascular endothelial cells mediate the recruitment of neural stem cells to the neurovascular niche. *Brain Res.* **2009**, *1268*, 24–37.

(34) Magge, S. N.; Malik, S. Z.; Royo, N. C.; Chen, H. I.; Yu, L.; Snyder, E. Y.; O'Rourke, D. M.; Watson, D. J. Role of monocyte chemoattractant protein-1 (MCP-1/CCL2) in migration of neural progenitor cells toward glial tumors. *J. Neurosci. Res.* **2009**, *87* (7), 1547–55.

(35) Ahmed, A. U.; Thaci, B.; Alexiades, N. G.; Han, Y.; Qian, S.; Liu, F.; Balyasnikova, I. V.; Ulasov, I. Y.; Aboody, K. S.; Lesniak, M. S. Neural Stem Cell-based Cell Carriers Enhance Therapeutic Efficacy of an Oncolytic Adenovirus in an Orthotopic Mouse Model of Human Glioblastoma. *Mol. Ther.* **2011**, doi: 10.1038/mt.2011.100.

(36) Xu, Q.; Yuan, X.; Xu, M.; McLafferty, F.; Hu, J.; Lee, B. S.; Liu, G.; Zeng, Z.; Black, K. L.; Yu, J. S.; Chemokine, C. X. C. receptor 4--mediated glioma tumor tracking by bone marrow--derived neural progenitor/stem cells. *Mol. Cancer Ther.* **2009**, *8* (9), 2746–53.

(37) Guan, Y.; Jiang, Z.; Ciric, B.; Rostami, A. M.; Zhang, G. X. Upregulation of chemokine receptor expression by IL-10/IL-4 in adult neural stem cells. *Exp. Mol. Pathol.* **2008**, *85* (3), 232–6.

(38) Shi, Y.; Hu, G.; Su, J.; Li, W.; Chen, Q.; Shou, P.; Xu, C.; Chen, X.; Huang, Y.; Zhu, Z.; Huang, X.; Han, X.; Xie, N.; Ren, G. Mesenchymal stem cells: a new strategy for immunosuppression and tissue repair. *Cell Res.* **2010**, *20* (5), 510–8.

(39) Fainstein, N.; Vaknin, I.; Einstein, O.; Zisman, P.; Ben Sasson, S. Z.; Baniyash, M.; Ben-Hur, T. Neural precursor cells inhibit multiple inflammatory signals. *Mol. Cell. Neurosci.* **2008**, *39* (3), 335–41.

(40) Jones, B. J.; McTaggart, S. J. Immunosuppression by mesenchymal stromal cells: from culture to clinic. *Exp. Hematol.* **2008**, *36* (6), 733–41.

(41) Ahmed, A. U.; Rolle, C. E.; Tyler, M. A.; Han, Y.; Sengupta, S.; Wainwright, D. A.; Balyasnikova, I. V.; Ulasov, I. V.; Lesniak, M. S. Bone Marrow Mesenchymal Stem Cells Loaded With an Oncolytic Adenovirus Suppress the Anti-adenoviral Immune Response in the Cotton Rat Model. *Mol. Ther.* **2010**.

(42) Ferguson, S. D.; Ahmed, A. U.; Thaci, B.; Mercer, R. W.; Lesniak, M. S. Crossing the boundaries: stem cells and gene therapy. *Discovery Med.* **2010**, *9* (46), 192–6.

(43) Aboody, K. S.; Najbauer, J.; Danks, M. K. Stem and progenitor cell-mediated tumor selective gene therapy. *Gene Ther.* **2008**, *15* (10), 739–52.

(44) Li, T. S.; Kubo, M.; Ueda, K.; Murakami, M.; Ohshima, M.; Kobayashi, T.; Tanaka, T.; Shirasawa, B.; Mikamo, A.; Hamano, K. Identification of risk factors related to poor angiogenic potency of bone marrow cells from different patients. *Circulation* **2009**, *120* (11 Suppl.), S255–61.

(45) Thu, M. S.; Najbauer, J.; Kendall, S. E.; Harutyunyan, I.; Sangalang, N.; Gutova, M.; Metz, M. Z.; Garcia, E.; Frank, R. T.; Kim, S. U.; Moats, R. A.; Aboody, K. S. Iron labeling and pre-clinical MRI visualization of therapeutic human neural stem cells in a murine glioma model. *PLoS One* **2009**, *4* (9), e7218.